SPACE SURVEILLANCE OBSERVATIONS AT THE AIUB ZIMMERWALD OBSERVATORY

J. Herzog, T. Schildknecht, A. Hinze, M. Ploner, and A. Vananti

Astronomical Institute, University of Bern, 3012 Bern, Switzerland, Email: {herzog, schildknecht, hinze, ploner, vananti}@aiub.unibe.ch

ABSTRACT

At the Zimmerwald observatory optical observations of artificial space objects are performed with the $1\,\mathrm{m}$ Laser and Astrometry Telescope, ZIMLAT, and the Small Robotic Telescope, ZimSMART. While ZIMLAT is used for follow-up observations of small-size space debris objects to maintain their orbits and determine physical characteristics, the main objective of ZimSMART is to perform systematic surveys of high-altitude orbit regions, in particular of the geostationary ring (GEO). The goal of these observations is to build-up and maintain orbit catalogues of objects in high-altitude orbits, including a catalogue of small-size debris with high area-to-mass ratios. Orbits from these catalogues are used to routinely track and characterize space debris with ZIMLAT, e. g. by means of light curve measurements.

One essential task of the space debris research is to find and understand the sources of debris, which in turn will enable to devise efficient mitigation measures – a prerequisite for the sustainable use of outer space. This paper will present the individual campaigns to detect, observe and characterise space debris objects. We will focus on survey observations of the Geostationary Ring and the MEO region performed by ZimSMART, and follow-up as well as light curve observations by ZIMLAT.

Key words: Zimmerwald Observatory; Space Surveillance.

1. THE ZIMMERWALD OBSERVATORY

The Zimmerwald Observatory is located $10\,\mathrm{km}$ South of Bern (Switzerland). Currently optical observations are performed with the $1\,\mathrm{m}$ Laser and Astrometric Telescope, ZIMLAT (Fig. 1(a)) and the $0.2\,\mathrm{m}$ Small Aperture Robotic Telescope, ZimSMART (Fig. 1(b)). Both telescopes are equipped with state-of-the-art CCD cameras with low readout-noise and high quantum efficiency. In Zimmerwald, three different types of cameras are used (see Tab. 1), which are exchanged on a regular basis to perform maintenance operations.

ZIMLAT (installed in 1997) is used either for laser ranging to satellites (SLR) or for optical observation of positions and magnitudes of near-Earth objects. During daytime the system operates in SLR mode only. During night time the available observation time is shared between SLR and CCD using negotiated priorities. The switching between the modes is done under computer control and needs less than half a minute. In addition light curves and photometric observations can be acquired.

Due to the large field of view (FoV), ZimSMART (installed in 2006) is best suited for sky surveys. The goals of these surveys are mainly to build-up and maintain a catalogue of artificial satellites and space debris objects (see [3, 4, 5] for details). Although routine operations are performed, the system is kept in an experimental state to test new software and hardware as well as new observation strategies.

2. ASTROMETRIC OBSERVATIONS

2.1. ZIMLAT Observations

ZIMLAT is especially used for follow-up observations of newly detected small-size space debris objects. These objects were either discovered by the ESA space debris telescope in Tenerife (see [6], campaign hprsat) or by observatories of our international partners, in particular the International Scientific Optical Network ISON led by the Keldysh Institute of Applied Mathematics KIAM (see [1], campaign ESAjointsat). The resulting positions and orbital elements are shared among the partners. ZIMLAT observations play a key role in the maintenance of orbits of objects with high area-to-mass ratios. Since 2005, follow-up observations of 303 objects discovered by the ESA space debris telescope were performed. We could also perform follow-up observations of 169 objects from ISON. Without these observations it would be impossible to build-up a catalogue of these objects. In addition observations objects in the USSTRATCOM catalogue were performed for scientific studies (campaigns longgeo and gto_long) and calibration (campaign GNSS). The composition of all campaigns is shown in Fig. 3. The magnitude distribution of all observations (Fig. 2) shows a signifi-

Proc. '6th European Conference on Space Debris'
Darmstadt, Germany, 22–25 April 2013 (ESA SP-723, August 2013)

Table 1. Properties of the cameras used at the telescopes in Zimmerwald

	SI1000	FLI09000	FLI16803
Chip	E2V 230-42EI	PL09000	PL16803
Chip dimension	$27.6\,\mathrm{mm} \times 30.7\,\mathrm{mm}$	$36.6\,\mathrm{mm} \times 36.6\,\mathrm{mm}$	$36.6\,\mathrm{mm} \times 36.6\,\mathrm{mm}$
Chip size in pixels	2048×2064	3056×3056	4096×4096
Max. quantum efficiency	$95\,\%$	$65\,\%$	$60\,\%$
Read-out noise	$\geq 5\,\mathrm{e}^-$	$12\,\mathrm{e}^-$	$10\,\mathrm{e}^-$

(a) ZIMLAT

(b) ZimSMART

Figure 1. The telescopes at the Zimmerwald observatory

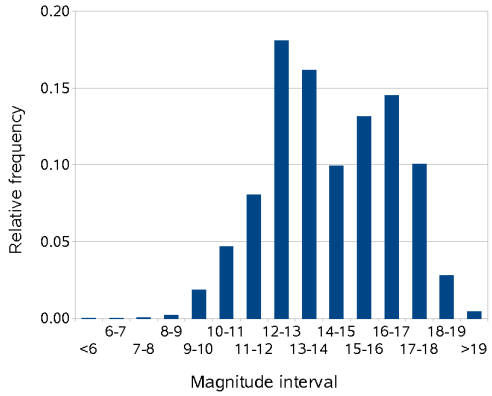

Figure 2. Apparent magnitude distribution of observations with ZIMLAT

cant decrease in the number of observations fainter than 17mag. This decrease is caused by the limiting magnitude of the optical system (about 19mag). The peak in the interval between 12 and 13mag may be induced by abandoned but intact satellites.

2.2. ZimSMART Observations

The main tasks of the ZimSMART telescope are survey observations of the GEO and Medium Earth Orbits (MEO) regions. GEO surveys are performed by scanning declination stripes with constant right ascension. Each stripe consists of 5 fields, so each stripe has a size of $4 \times 20\,\mathrm{deg}^2$. During the acquisition the telescope is looking in a direction fixed with respect to the Earth. For each field there are 5 images taken with an exposure time of 7 seconds. The time difference between the acquisitions of each stripe is about 15 minutes. The images are analysed with an automated procedure to find any moving object. Astrometric positions and apparent magnitudes are determined for each detection of a moving object. Observations on consecutive frames are listed to form so-called tracklets. Since June 2008, more than 129140 tracklets have been found. This number is not identical with the number of objects due to the fact that more than one tracklet can belong to the same object. The decrease in the magnitude distribution (Fig. 4) is again caused by the limiting magnitude of the optical system (about $13.5\,\mathrm{mag}$).

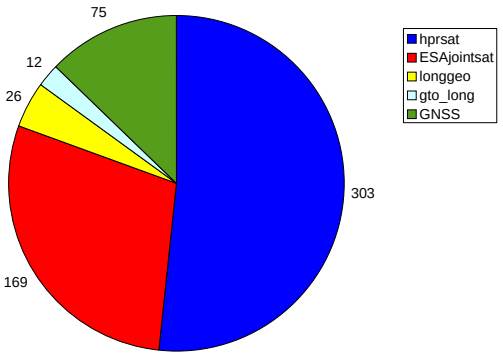

Figure 3. Number of objects observed by ZIMLAT, separated into different campaigns

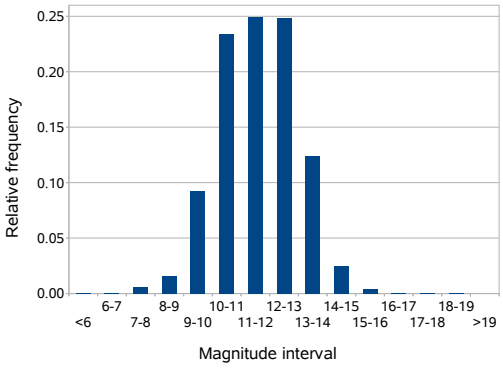

Figure 4. Apparent magnitude distribution of the GEO survey observations with ZimSMART

2.3. Accuracy of Optical Satellite Observations

The accuracy of astrometric observations of objects depends mainly on the accuracy of the parameters of the inner and exterior orientation of the image and the accuracy of the measured positions of the objects relative to reference stars. For objects moving with respect to the sky background the recording of the exact starting and end epoch of the exposures is crucial. Errors in the exposure epoch induce errors in the measured position (essentially in alongtrack direction). For geostationary satellites an error of $7\,\mathrm{ms}$ causes an alongtrack error of $0.1''$, which is of the same order as the RMS of the astrometric positions of ZIMLAT. For satellites in lower orbits the errors are even higher. This accuracy can hardly be achieved by taking the shutter command signals as references for the exposure epoch due to the following reasons: On one hand the delay between sending a signal for opening and closing the shutter and the reaction of the shutter may vary with the ambient air temperature, on the other hand the time for opening and closing will probably not be identical. This asymmetry results in different midexposure epochs depending on the distance from the centre of the image.

For ZimSMART the requirement for the epoch registration accuracy is lower by a factor of 7 (about $45\,\mathrm{ms}$) due to the higher RMS of the astrometric positions ($0.7''$) in comparison to observations of ZIMLAT ($0.1''$). Astrometric positions of GNSS satellites are compared to precise ephemerides based on microwave observations to calibrate the epoch registration. The comparisons indicated a systematic offset in alongtrack direction of the ZimSMART observations caused by systematic errors in the recording of the exposure epochs of 0.03 seconds. This offset is caused by the delay between sending a signal for opening and closing the shutter and the reaction of the shutter. After taking this delay into consideration the maximum difference in right ascension and declination does not exceed $\pm 1.5''$ for ZIMLAT observations (Fig. 5(a)) and $\pm 10''$ for ZimSMART observations (Fig. 5(b)).

2.4. Long-time Modelling of Orbits

EUMETSAT's weather satellites MSG$-$2 was launched from Kourou, French Guiana on December 22, 2005. Just prior to reaching operational altitude the cooler cover was ejected in a special manoeuvre, several hundred kilometres away from the geostationary orbital plane, ensuring that they cannot come into contact with other operational satellites. On January 4, 2006 AIUB successfully aquired first observations of the cooler cover. During the observation the telescope was looking in a direction fixed with respect to the Earth. The cooler cover appears as dot as it is nearly stationary with respect to the Earth rotation. The stars appear as streaks (Fig. 6).

For the maintenance of a catalogue long-time modelling of orbits is of special interest. The better an orbit can

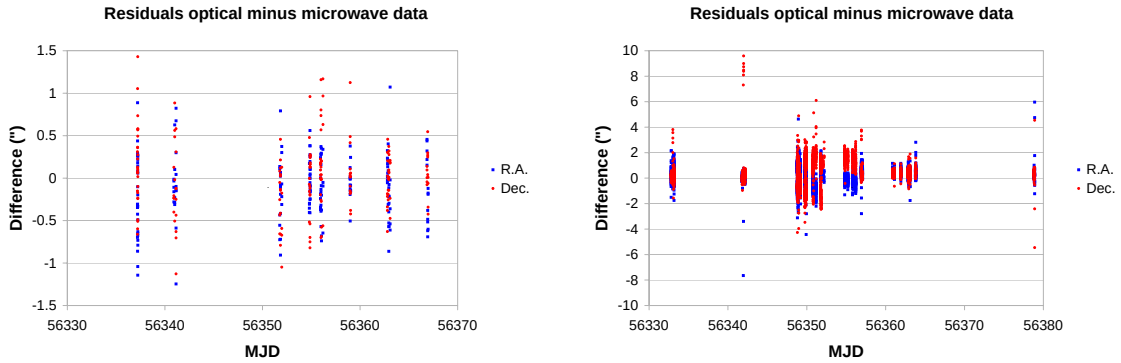

(a) Observations of ZIMLAT

(b) Observations of ZimSMART

Figure 5. Difference of astrometric observations and high precision ephemerides based on observations in right ascension (R.A.) and declination (Dec.) for a set ofGPS Satellites

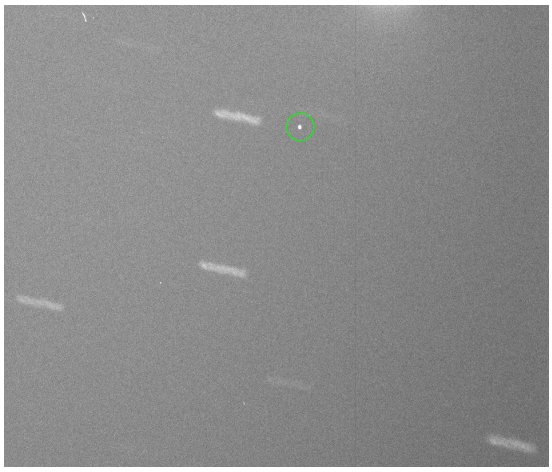

Figure 6. Image of the cooler cover (05049E) of MSG−2, marked by the green circle

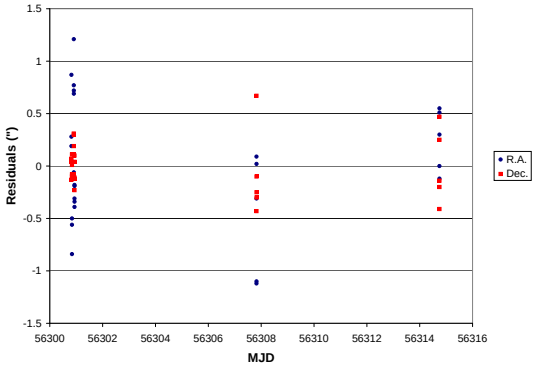

Figure 7. Residuals of an orbit determination of 05049E with an arc length of two weeks

be modelled the longer may be the time interval between follow-up observations. Beside the six osculating elements, additional model parameters are considered in the orbit determination.

These parameters are mainly the direct solar radiation pressure and the accelerations in alongtrack direction. Two examples of long-arc orbit fits for the MSG−2 cooler cover are given in the Figs. 7 and 8.The orbital parameters are shown in the Tabs. 2 and 3, and were both modelled with the program SATORB (described in detail in [2]).

The following a priori force field was used:

- Earth potential up to degree and order 12
- Gravitational attraction from Sun and Moon
- Earth tides

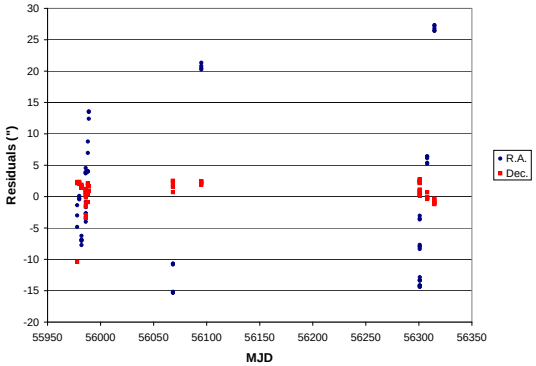

Figure 8. Residuals of an orbit determination of 05049E with an arc length of eleven months

Table 2. Orbital parameters of 05049E with an arc length of two weeks

```
OSCULATING ELEMENTS AND THEIR RMS ERRORS
*************************************************
OSCULATION EPOCH = 56300.8192101 MJD
SEMIMAJOR AXIS   =  41917197.523 M   +-       4.344 M
REV. PERIOD U    =      1423.469 MIN
ECCENTRICITY     =  0.0008575675 --- +-0.0000043738
INCLINATION      =     4.9448521 DEG +- 0.000117158
R.A. OF NODE     =    73.5699707 DEG +- 0.000630385
ARG OF PERIGEE   =   131.4186486 DEG +- 0.649488564
ARG OF LAT AT T0 =   315.2591887 DEG +- 0.000639133
*************************************************
PARAMETER = DRP  VALUE =0.985021D+00 +-0.352344D-01
*************************************************
RMS=   0.47"
```

Table 3. Orbital parameters of 05049E with an arc length of about 337 days

```
OSCULATING ELEMENTS AND THEIR RMS ERRORS
*************************************************
OSCULATION EPOCH = 55977.8971264 MJD
SEMIMAJOR AXIS   =  41917822.640 M   +-       4.683 M
REV. PERIOD U    =      1423.501 MIN
ECCENTRICITY     =  0.0004243693 --- +-0.0000143177
INCLINATION      =     4.2273997 DEG +- 0.000469172
R.A. OF NODE     =    79.3187330 DEG +- 0.004938110
ARG OF PERIGEE   =  -290.7620344 DEG +- 1.847914594
ARG OF LAT AT T0 =    56.8312773 DEG +- 0.004963384
*************************************************
PARAMETER = DRP  VALUE =0.268637D+00 +-0.217395D-01
*************************************************
RMS=   8.87"
```

- Direct radiation pressure

The following parameters were estimated:

- Six Keplerian elements
- Scaling factor for direct radiation pressure (DRP)
- Along track acceleration (S)
- Once per revolution terms in along track direction (SC, SS)

In both cases the rms error of a single observation ($0.5''$ resp. $8.9''$) is significantly larger than the measurement noise of $0.2''$, due to an insufficient radiation pressure model and a missing attitude motion model. Although the orbit model cannot represent the observations correctly, the object will be inside the field of view of ZIMLAT even when no follow-up observations can be performed for several months.

3. PHOTOMETRIC OBSERVATIONS – LIGHT CURVE MEASUREMENTS

During the searches for debris in the geostationary transfer orbit region a new population of objects has been found in unexpected orbits where no potential progenitors exist (see [8]). Temporally resolved photometry

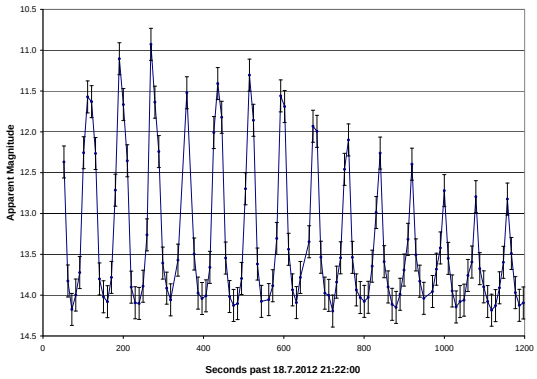

(a) E10040A $\left(\mathrm{AMR} = 0.007\,\mathrm{m^2\,kg^{-1}}\right)$

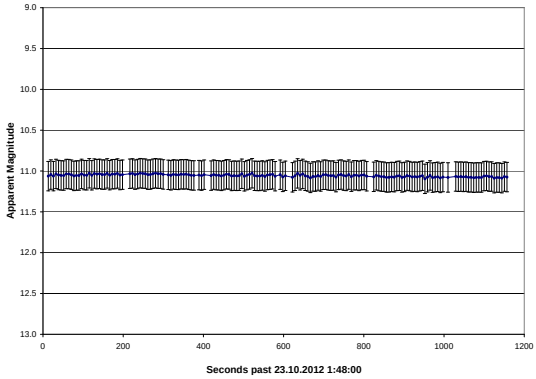

(b) 11035D (Breeze-M R/B)

Figure 9. Examples of light curves

(light curves) have been acquired with the ZIMLAT telescope to study the nature of these debris (see [7]). The light curves were obtained by taking series of small subframes centred on the object with an exposure time of a few seconds. On these subframes the intensity of the object is measured without any reduction like dark or flat field correction. Some light curves show strong variations over short time intervals (Fig. 9(a)) where others do not (Fig. 9(b)). For a better comparability, the graphs have the same dimension on magnitude scale.

REFERENCES

1. Vladimir Agapov et al. The ISON International Observation Network – Latest Scientific Achievements and the Future Works. In *Proceedings of the* 37^{th} *COSPAR Scientific Assembly*, 2008.
2. Gerhard Beutler. *Methods of Celestial Mechanics*. Springer-Verlag, Heidelberg, 2005.
3. Johannes Herzog et al. Build-up and maintenance of a catalogue of GEO objects with ZimSMART and ZimSMART 2. In *Proceedings of the* 61^{st} *International Astronautical Congress*, 2010.
4. Johannes Herzog et al. Space Debris Observations

with ZimSMART. In *Proceedings of the European Space Surveillance Conference*, 2011.

5. Johannes Herzog and Thomas Schildknecht. Search for space debris in the MEO region with ZimSMART. In *Proceedings of the* 63^{rd} *International Astronautical Congress*, 2012.
6. Thomas Schildknecht et al. Optical Observations of Space Debris in High-Altitude Orbits. In *Proceedings of the Fourth European Conference on Space Debris*, 2005.
7. Thomas Schildknecht et al. Color Photometry and Light Curve Observations of Space Debris in GEO. In *Proceedings of the* 59^{th} *International Astronautical Congress*, 2008.
8. Thomas Schildknecht et al. Properties of the High Area-to-Mass Ratio Space Debris Population at High Altitudes. *Advances in Space Research*, 41:1039–1045, 2008.